

# Steady state solution of NFC model with nonlinear load using PEEC

Samuel Kvasnicka and Thomas Bauernfeind

*Institute of Fundamentals and Theory in Electrical Engineering,  
Faculty of Electrical and Information Engineering,  
Graz University of Technology, Graz, Austria and Silicon Austria Labs,  
TU-Graz SAL GEMC Lab, Graz, Austria*

Paul Baumgartner

*Institute of Fundamentals and Theory in Electrical Engineering,  
Faculty of Electrical and Information Engineering,  
Graz University of Technology, Graz, Austria, and*

Riccardo Torchio

*Dipartimento di Ingegneria Industriale, Universita degli Studi di Padova,  
Padova, Italy*

## Abstract

**Purpose** – The purpose of this paper is to show that the computation of time-periodic signals for coupled antenna-circuit problems can be substantially accelerated by means of the single shooting method. This allows an efficient analysis of nonlinearly loaded coupled loop antennas for near field communication (NFC) applications.

**Design/methodology/approach** – For the modelling of electrically small coupled field-circuit problems, the partial element equivalent circuit (PEEC) method shows to be very efficient. For analysing the circuit-like description of the coupled problem, this paper developed a generalised modified nodal analysis (MNA) and applied it to specific NFC problems.

**Findings** – It is shown that the periodic steady state (PSS) solution of the resulting differential-algebraic system can be computed very time efficiently by the single shooting method. A speedup of roughly 114 to conventional transient approaches can be achieved.

**Practical implications** – The proposed approach appears to be an efficient alternative for the computation of time PSS solutions for nonlinear circuit problems coupled with discretised conductive structures, where the homogeneous solution is not of interest.

**Originality/value** – The present paper explores the implementation and application of the shooting method for nonlinearly loaded coupled antenna-circuit problems based on the PEEC method and shows the efficiency of this approach.

**Keywords** Circuit analysis, Transient analysis, Time-domain modelling, Equivalent circuit model, Computational electromagnetics, Field circuit models, Near field communication, Nonlinear resistive loads, Full-wave rectifier, Partial element equivalent circuit method, Modified nodal analysis, Differential-algebraic equation, Backward differentiation formula, Single shooting method

**Paper type** Research paper



## 1. Introduction

Before introducing a near field communication (NFC) device on the market, a rather large number of standardisation tests have to be carried out, which are time-consuming, expensive and require a prototype device. To overcome this problem, the idea is to develop a digital twin of the NFC device and carry out those tests in terms of numerical simulations, as e.g. proposed in (Bauernfeind *et al.*, 2020, pp. 3–14), which rely on a frequency domain method. On the other hand, the NFC-IC as well as the standardised test equipment, show a strong nonlinear electric behaviour. Hence, accurate modelling of this nonlinear electric behaviour is not possible with this approach. Consequently, a strategy is needed which allows the incorporation of this behaviour. Because we are interested in the periodic steady state (PSS) solution only, we propose to apply the single shooting method, for instance, (Kundert *et al.*, 1990, pp. 65–70) or (Kvasnicka 2020, pp. 42–45), which solves the underlying differential-algebraic equation (DAE) in terms of a boundary value problem (BVP) instead of an initial value problem (IVP) as in conventional transient solution strategies.

Like in (Bauernfeind *et al.*, 2018), the partial element equivalent circuit (PEEC) method is applied, which is a useful method to model electromagnetic (EM) field problems in terms of a circuit-like description. Hence, it is possible to combine an EM problem with external lumped circuits which contain linear and nonlinear elements. Thus, numerical techniques, which are applicable in the electric circuit analysis, can also be applied to such hybrid EM and circuit models to compute the PSS solution.

For the discretisation of the loop structures, one-dimensional (1D) stick elements are used, which significantly simplifies the modelling of the NFC loop antennas. However, the adoption of this kind of element introduces unavoidable approximations. Indeed, skin effects are completely neglected. Moreover, only volume electric charge density is considered. This may lead to some inaccuracies when capacitive effects between close conductive surfaces are predominant (Torchio, 2019). However, the PEEC method with stick wires allows for a good trade-off between accuracy and computational costs, especially in the optimisation-based pre-design phase.

The remainder of the paper is structured as follows. In Section 2, the PEEC-based model of the coupled field-circuit problem is explained. Here, special attention is paid to the needed modification of the resulting system matrix of the PEEC formulation to enable the applicability of the modified nodal analysis (MNA) on the circuit representation of the coupled field-circuit problem. This modification allows the coupling with external nonlinear circuit elements in a standardised MNA formulation, which results in a description via DAE system. In Section 3, the solution strategies transient analysis and single shooting based on backward differentiation formula (BDF) are introduced and briefly discussed. Section 4 shows the simulation results of the test problem consisting of two close-coupled NFC loop antennas with nonlinear resistive loading. Finally, in Section 5, a conclusion of the obtained results, as well as an outlook on future work, is presented.

## 2. Modelling

### 2.1 Modelling conductive structures using PEEC method

A quasi-static PEEC method is used to model the conductive domain, whereby in the applied PEEC formulation, neither dielectric nor magnetic materials are considered, which is no major restriction regarding the NFC standardisation tests.

The conductive structure, e.g. NFC antennas, can be discretised by  $b_{L,\text{peec}}$  thin wire stick elements which are modelled by  $b_{L,\text{peec}}$  PEEC cells and  $n_{C,\text{peec}}$  PEEC nodes. Figure 1 shows the  $m$ -th PEEC cell between the nodes  $i$  and  $j$  (Ekman, 2003, p. 32 and p. 54), whereby the PEEC cells are described by a symmetric partial potential matrix  $\mathbf{P} = (p_{ij})_{1 \leq i, j \leq n_{C,\text{peec}}}$ , a

partial inductance matrix  $\mathbf{L}' = (L'_{ij})_{1 \leq i, j \leq b_{L, \text{peec}}}$  and a diagonal partial resistance matrix  $\mathbf{R}' = \text{diag}(R'_1, \dots, R'_{b_{L, \text{peec}}})$ . In general, the matrices  $\mathbf{P}$  and  $\mathbf{L}'$  are fully populated. In the case of filamentary coils, the coefficients of the matrices  $\mathbf{P}$ ,  $\mathbf{L}'$  and  $\mathbf{R}'$  can be computed according to (Torchio *et al.*, 2017, p. 2), which corresponds to a 1D discretisation approach.

For solving the circuit description given by the PEEC method, the MNA is used. Hence, it is useful to model the capacitive elements shown in Figure 1 in a different way. The diagonal matrix

$$\mathbf{F} := \text{diag}\left(\frac{1}{p_{1,1}}, \dots, \frac{1}{p_{n_{C, \text{peec}}, n_{C, \text{peec}}}}\right)$$

contains the (pseudo-) capacitances  $C'_i$  regarding Figure 1. The matrices  $\mathbf{P}$  and  $\mathbf{F}$  are invertible, and therefore the invertible matrix  $\mathbf{S} := \mathbf{P} \cdot \mathbf{F}$  can be defined. Due to the symmetry of  $\mathbf{P}$ , the relation  $\mathbf{F} \cdot \mathbf{S}^{-1} = \mathbf{P}^{-1} = (\mathbf{S}^T)^{-1} \cdot \mathbf{F}$  is valid. With respect to Figure 1 and the definition of the PEEC node potentials  $\mathbf{e}_{C, \text{peec}}(t) := (e_1(t), \dots, e_{n_{C, \text{peec}}}(t))^T$ , the branch voltages  $\mathbf{u}_{C'}(t) = (u_{C'_1}(t), \dots, u_{C'_{n_{C, \text{peec}}}}(t))^T$  of the (pseudo-) capacitances can be written as

$$\mathbf{u}_{C'}(t) = \mathbf{S}^{-1} \cdot \mathbf{e}_{C, \text{peec}}(t).$$

Consequently, the matrices  $\mathbf{C}_{\text{peec}} := (\mathbf{S}^T)^{-1} \cdot \mathbf{F}$  and  $\mathbf{L}_{\text{peec}} := \mathbf{L}'$  can be defined. Figure 2 shows an equivalent representation of the  $m$ -th PEEC cell with respect to Figure 1, consisting of coupled inductances  $\mathbf{L}_{\text{peec}, m}^T$  and coupled capacitances  $\mathbf{C}_{\text{peec}, i}^T$ ,  $\mathbf{C}_{\text{peec}, j}^T$  whereby  $\mathbf{L}_{\text{peec}, m}^T$  and  $\mathbf{C}_{\text{peec}, i}^T$  denotes the  $m$ -th and  $i$ -th row vectors of the matrices  $\mathbf{L}_{\text{peec}}$  and  $\mathbf{C}_{\text{peec}}$ , respectively.

**Figure 1.**  
Circuit representation of the  $m$ -th PEEC cell. The voltage sources in the cell represent the capacitive and inductive coupling to other PEEC cells

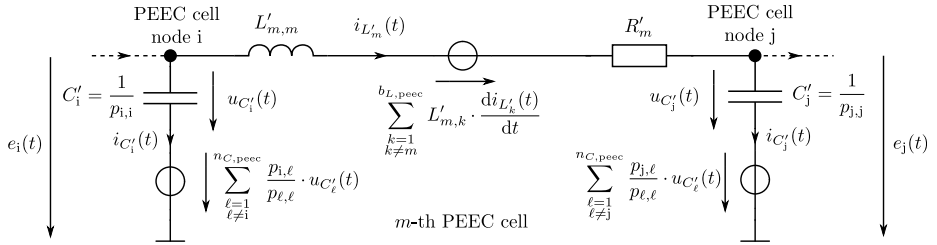
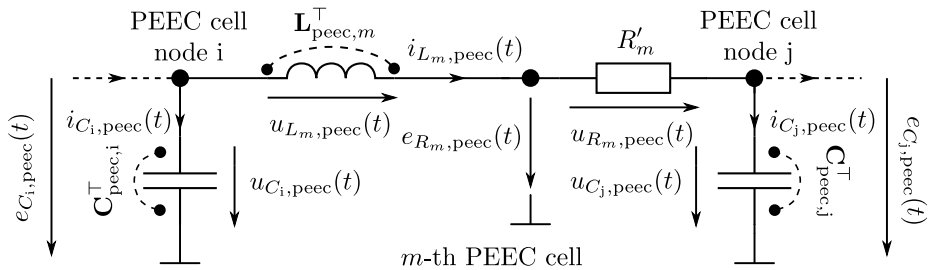


**Figure 2.**  
Equivalent circuit representation of the  $m$ -th PEEC cell used in the MNA approach



Regarding Figure 2, the relations between capacitive and inductive branch currents and voltages are given by

$$\begin{aligned}\mathbf{i}_{C,\text{peec}}(t) &= \mathbf{C}_{\text{peec}} \cdot \frac{d\mathbf{u}_{C,\text{peec}}(t)}{dt}, \\ \mathbf{u}_{L,\text{peec}}(t) &= \mathbf{L}_{\text{peec}} \cdot \frac{d\mathbf{i}_{L,\text{peec}}(t)}{dt},\end{aligned}$$

which also considers the capacitive and inductive coupling between the cells.

## 2.2 Applying MNA using PEEC model

Due to the circuit-like description of the EM field problem by means of the PEEC method, external lumped elements can be easily added. In the proposed MNA formulation, linear resistive, capacitive and inductive elements, nonlinear resistive elements such as diodes and independent sources can be considered.

The external circuit to be analysed, possesses  $b_U$  independent voltage sources,  $b_I$  independent current sources,  $b_C := n_{C,\text{peec}} + b_{C,\text{ext}}$  linear capacitive elements,  $b_L := b_{L,\text{peec}} + b_{L,\text{ext}}$  linear inductive elements and  $b_R := b_{R,\text{peec}} + b_{R,\text{ext,lin}} + b_{R,\text{ext,NL}}$  resistive elements, whereby the subscripts “peec”, “ext”, “ext,lin” and “ext,NL” relates to elements of the PEEC cells, external elements, external linear and nonlinear elements, respectively. The common reference potential of the lumped circuit corresponds with the reference potential of the PEEC cells. The total number of nodes is indicated by  $n$  and  $n - 1 = n_{C,\text{peec}} + b_{L,\text{peec}} + b_{L,\text{ext}} + n_{\text{ext}}$  complies with the total number of nodes excluding the reference node. Here,  $n_{C,\text{peec}}$  corresponds to the PEEC nodes,  $b_{L,\text{peec}}$  corresponds to the added node between the inductive and resistive element of each PEEC cell (Figure 2), and  $n_{\text{ext}}$  corresponds to the additional nodes of the external lumped circuit.

In the MNA, the topology of the whole circuit is described by the reduced incidence matrix  $\mathbf{A}$ , for instance (Riaza, 2008, p. 198) or (Kvasnicka, 2020, pp. 18–19), consisting of blocks for the different types of circuit elements

$$\mathbf{A} := (\mathbf{A}_R, \mathbf{A}_C, \mathbf{A}_L, \mathbf{A}_U, \mathbf{A}_I),$$

where  $\mathbf{A}_\ell \in \mathbb{R}^{(n-1) \times b_\ell}$  for  $\ell \in \{R, C, L, U, I\}$  is introduced. Further, the resistive, capacitive and inductive reduced incidence matrices are subdivided into

$$\begin{aligned}\mathbf{A}_R &:= (\mathbf{A}_{R,\text{peec}}, \mathbf{A}_{R,\text{ext,lin}}, \mathbf{A}_{R,\text{ext,NL}}), \\ \mathbf{A}_C &:= (\mathbf{A}_{C,\text{peec}}, \mathbf{A}_{C,\text{ext}}), \\ \mathbf{A}_L &:= (\mathbf{A}_{L,\text{peec}}, \mathbf{A}_{L,\text{ext}}),\end{aligned}$$

relating to the appropriate elements. For example, the  $k$ -th column of  $\mathbf{A}_{C,\text{ext}}$  describes the incidence between the branch of the  $k$ -th external capacitance and the connected nodes. The connection between branch voltages  $\mathbf{u}(t)$  and node potentials  $\mathbf{e}(t)$  is then given as

$$\mathbf{u}(t) - \mathbf{A}^\top \cdot \mathbf{e}(t) = \mathbf{0}.$$

The relation between the external linear resistive, capacitive and inductive elements are described by their characteristic equations using matrices  $\mathbf{R}_{\text{ext,lin}} \in \mathbb{R}^{b_{R,\text{ext,lin}} \times b_{R,\text{ext,lin}}}$ ,  $\mathbf{C}_{\text{ext}} \in \mathbb{R}^{b_{C,\text{ext}} \times b_{C,\text{ext}}}$  and  $\mathbf{L}_{\text{ext}} \in \mathbb{R}^{b_{L,\text{ext}} \times b_{L,\text{ext}}}$ . The definition of the function  $\gamma_R : \mathbb{R}^{b_R} \rightarrow \mathbb{R}^{b_R}$

$$\boldsymbol{\gamma}_R \begin{pmatrix} \mathbf{u}_{R,\text{peec}} \\ \mathbf{u}_{R,\text{ext},\text{lin}} \\ \mathbf{u}_{R,\text{ext},\text{NL}} \end{pmatrix} := \begin{pmatrix} \mathbf{R}_{\text{peec}}^{-1} \cdot \mathbf{u}_{R,\text{peec}} \\ \mathbf{R}_{\text{ext},\text{lin}}^{-1} \cdot \mathbf{u}_{R,\text{ext},\text{lin}} \\ \boldsymbol{\gamma}_{R,\text{ext},\text{NL}}(\mathbf{u}_{R,\text{ext},\text{NL}}) \end{pmatrix},$$

describes the behaviour of resistive branch currents depending on the resistive branch voltages. Therefore, a function  $\boldsymbol{\gamma}_{R,\text{ext},\text{NL}} : \mathbb{R}^{b_{R,\text{ext},\text{NL}}} \rightarrow \mathbb{R}^{b_{R,\text{ext},\text{NL}}}$  describes the behaviour of the nonlinear resistive elements and  $\mathbf{R}_{\text{peec}} = \mathbf{R}'$  describes the behaviour of the PEEC of the PEEC resistance, in accordance with Section 2.1.

To avoid a MNA formulation including  $(\mathbf{S}^\top)^{-1}$ , the relation  $\mathbf{F} \cdot \mathbf{S}^{-1} = (\mathbf{S}^\top)^{-1} \cdot \mathbf{F}$  can be used, according to Section 2.1. Therefore, the matrices  $\tilde{\mathbf{S}}, \tilde{\mathbf{F}}$  are defined as

$$\begin{aligned} \tilde{\mathbf{S}} &:= \begin{pmatrix} \mathbf{S}^\top & \mathbf{0} \\ \mathbf{0} & \mathbf{I} \end{pmatrix} \in \mathbb{R}^{(n-1) \times (n-1)}, \\ \tilde{\mathbf{F}} &:= \begin{pmatrix} \mathbf{F}^\top & \mathbf{0} \\ \mathbf{0} & \mathbf{0} \end{pmatrix} \in \mathbb{R}^{(n-1) \times (n-1)}, \end{aligned}$$

whereby  $\mathbf{I}$  denote the identity matrix and  $\mathbf{0}$  denote the zero matrix.

Defining  $m := n - 1 + b_{L,\text{peec}} + b_{L,\text{ext}} + b_U$  and by taking the previous preliminaries into account, the MNA formulation can be applied, for instance, (Riaza 2008, p. 215) or (Kvasnicka 2020, pp. 67–68), resulting in the DAE as follows

$$\mathbf{M} \cdot \frac{d\mathbf{x}(t)}{dt} + \mathbf{f}(\mathbf{x}(t)) + \mathbf{b}(t) = \mathbf{0}. \quad (1)$$

Here,  $\mathbf{x}(t) := (\mathbf{e}(t)^\top, \mathbf{i}_L(t)^\top, \mathbf{i}_U(t)^\top)^\top \in \mathbb{R}^m$  is the vector of unknowns, consisting of node potentials  $\mathbf{e}(t) = (\mathbf{e}_{C,\text{peec}}(t)^\top, \mathbf{e}_{R,\text{peec}}(t)^\top, \mathbf{e}_{\text{ext}}(t)^\top)^\top$ , currents of independent voltage sources  $\mathbf{i}_U(t)$  and inductive currents  $\mathbf{i}_L(t) = (\mathbf{i}_{L,\text{peec}}(t)^\top, \mathbf{i}_{L,\text{ext}}(t)^\top)^\top$ .

The matrix  $\mathbf{M} \in \mathbb{R}^{m \times m}$ ,  $\mathbf{b} : \mathbb{R} \rightarrow \mathbb{R}^m$  and the relation  $\mathbf{f} : \mathbb{R}^{n-1} \times \mathbb{R}^{b_L} \times \mathbb{R}^{b_U} \rightarrow \mathbb{R}^m$  are defined as

$$\begin{aligned} \mathbf{M} &= \begin{pmatrix} \tilde{\mathbf{F}} + \tilde{\mathbf{S}} \cdot \mathbf{A}_{C,\text{ext}} \cdot \mathbf{C}_{\text{ext}} \cdot \mathbf{A}_{C,\text{ext}}^\top & \mathbf{0} & \mathbf{0} & \mathbf{0} \\ \mathbf{0} & \mathbf{L}_{\text{peec}} & \mathbf{0} & \mathbf{0} \\ \mathbf{0} & \mathbf{0} & \mathbf{L}_{\text{ext}} & \mathbf{0} \\ \mathbf{0} & \mathbf{0} & \mathbf{0} & \mathbf{0} \end{pmatrix}, \\ \mathbf{f} \begin{pmatrix} \mathbf{e} \\ \mathbf{i}_L \\ \mathbf{i}_U \end{pmatrix} &= \begin{pmatrix} \tilde{\mathbf{S}} \cdot (\mathbf{A}_R \cdot \boldsymbol{\gamma}_R(\mathbf{A}_R^\top \cdot \mathbf{e}) + \mathbf{A}_L \cdot \mathbf{i}_L + \mathbf{A}_U \cdot \mathbf{i}_U) \\ -\mathbf{A}_L^\top \cdot \mathbf{e} \\ \mathbf{A}_U^\top \cdot \mathbf{e} \end{pmatrix}, \\ \mathbf{b}(t) &= \begin{pmatrix} \tilde{\mathbf{S}} \cdot \mathbf{A}_I \cdot \mathbf{i}_Q(t) \\ \mathbf{0} \\ -\mathbf{u}_Q(t) \end{pmatrix}, \end{aligned}$$

with known functions  $\mathbf{i}_Q(t)$  and  $\mathbf{u}_Q(t)$  of independent current and voltage sources, respectively. Finally, a DAE description of the conductive structure coupled with an external circuit is given. Based on these relations, numerical methods are applied for obtaining the PSS solution.

### 3. Numerical methods

For numerically computing the PSS solution of equation (1), some requirements have to be fulfilled, which in the following are briefly summarised. Firstly, the complete circuit to be analysed is supplied by  $T$ -periodic sources, i.e.  $\mathbf{i}_Q(t)$  and  $\mathbf{u}_Q(t)$  are  $T$ -periodic functions. Secondly, because of the presence of nonlinear elements, it is assumed that the describing DAE (1) ensures a PSS solution. Thirdly, the quasilinear DAE (1) is at most an index-1 DAE, whereby an introduction for the DAE index can be found, for instance, in (Riaza 2008, pp. 5–8) or (Schwarz and Tischendorf 2005, pp. 7–8).

The computation of the PSS solution is implemented with a single shooting based on BDF. This linear multistep method is a stable algorithm for computing the solution of an index-1 DAE (Ascher and Petzold, 1998, pp. 266–267). In the case of DAEs with a higher index, a stable functionality of BDF cannot be guaranteed, and therefore, an index reduction technique is essential.

Section 3.1 introduces a transient analysis algorithm based on BDF3, which is a part of the single shooting algorithm in Section 3.2. In both subsections, a solution strategy is provided to solve nonlinear systems of equations using the local Newton method. To achieve a better convergence behaviour, for instance, the implementation of a damped Newton method is recommended. However, the essential calculations are provided from the local Newton method.

#### 3.1 Transient analysis using BDF3

Algorithm 1 (Kvasnicka, 2020, p. 40) is based on (Ascher and Petzold 1998, pp. 129–130 and pp. 266–267) and shows for a constant step-size  $h > 0$  an implementation to solve the IVP of the DAE (1) regarding a consistent initial value  $\mathbf{x}_0 = \mathbf{x}(0) \in \mathbb{R}^m$ . Here, BDF3 is used, whereby BDF1 and BDF2 are recursively used in the initial phase. The coefficients of BDF1 to BDF3 are noted as a comment in Algorithm 1, in accordance with (Ascher and Petzold, 1998, p. 130). One possibility to find  $\mathbf{x}_{n+1}$ , which fulfils the relationship in line 6 of Algorithm 1, is the application of the local Newton method (Kvasnicka, 2020, p. 40), which is presented in the following. Firstly, in accordance with DAE (1), the Jacobian matrix  $\mathbf{J}_f(\mathbf{x}) \in \mathbb{R}^{m \times m}$  with  $\mathbf{x} := (\mathbf{e}^\top, \mathbf{i}_L^\top, \mathbf{i}_U^\top)^\top$ , is given as

$$\mathbf{J}_f(\mathbf{x}) = \begin{pmatrix} \tilde{\mathbf{S}} \cdot \mathbf{A}_R \cdot \mathbf{J}_{\gamma_R}(\mathbf{A}_R^\top \cdot \mathbf{e}) \cdot \mathbf{A}_R^\top & \tilde{\mathbf{S}} \cdot \mathbf{A}_L & \tilde{\mathbf{S}} \cdot \mathbf{A}_U \\ -\mathbf{A}_L^\top & \mathbf{0} & \mathbf{0} \\ \mathbf{A}_U^\top & \mathbf{0} & \mathbf{0} \end{pmatrix}. \quad (2)$$

Here,  $\mathbf{J}_{\gamma_R}(\mathbf{A}_R^\top \cdot \mathbf{e})$  denotes the Jacobian matrix of the function  $\gamma_R$ , evaluated in the point  $\mathbf{A}_R^\top \cdot \mathbf{e}$ .

Secondly, the function  $\mathbf{F} : \mathbb{R}^m \rightarrow \mathbb{R}^m$  with

$$\mathbf{F}(\mathbf{x}_{n+1}) = \left[ \frac{1}{\beta_0 \cdot h} \cdot \sum_{k=0}^K (\alpha_k \cdot \mathbf{M} \cdot \mathbf{x}_{n+1-k}) \right] + \mathbf{f}(\mathbf{x}_{n+1}) + \mathbf{b}(t_{n+1}),$$

is defined for  $K \in \{1,2,3\}$  and the BDF coefficients as given in Algorithm 1. It can be proven that

$$\mathbf{J}_F(\mathbf{x}) = \frac{\alpha_0}{\beta_0 \cdot h} \cdot \mathbf{M} + \mathbf{J}_f(\mathbf{x})$$

is the Jacobian matrix of  $\mathbf{F}$  in  $\mathbf{x}$ . Consequently, applying the local Newton method to solve  $\mathbf{F}(\mathbf{x}_{n+1}) = \mathbf{0}$ , the  $(\ell + 1)$ -th iterated approximation of  $\mathbf{x}_{n+1}$ , is given as

$$\mathbf{x}_{n+1}^{(\ell+1)} = \mathbf{x}_{n+1}^{(\ell)} - \left( \mathbf{J}_F(\mathbf{x}_{n+1}^{(\ell)}) \right)^{-1} \cdot \mathbf{F}(\mathbf{x}_{n+1}^{(\ell)}).$$

Further, for example, the initial value  $\mathbf{x}_{n+1}^{(0)} = \mathbf{x}_n$  can be chosen in the first Newton iteration, depending on the solution  $\mathbf{x}_n$  in the previous time step.

---

**Algorithm 1:** Solve DAE-IVP using BDF3

---

**Input:** DAE (1),  $\mathbf{x}_0$ ,  $h > 0$ ,  $t_0 = 0, \dots, t_N = N \cdot h$   
**Output:** Computed solution  $\mathbf{x}_1, \dots, \mathbf{x}_N$

```

1 for  $n \leftarrow 0, \dots, N - 1$  do
2   if  $(n + 1) < 3$  then
3      $K \leftarrow n + 1$ 
4   else
5      $K \leftarrow 3$ 
6     //  $K = 1$ :  $\beta_0 = 1, \alpha_0 = 1, \alpha_1 = -1$ 
7     //  $K = 2$ :  $\beta_0 = \frac{2}{3}, \alpha_0 = 1, \alpha_1 = -\frac{4}{3}, \alpha_2 = \frac{1}{3}$ 
8     //  $K = 3$ :  $\beta_0 = \frac{6}{11}, \alpha_0 = 1, \alpha_1 = -\frac{18}{11}, \alpha_2 = \frac{9}{11}, \alpha_3 = -\frac{2}{11}$ 
9     // Compute  $\mathbf{x}_{n+1}$ , for instance with a (damped) Newton method
10     $\mathbf{0} = \frac{1}{\beta_0 \cdot h} \cdot \sum_{k=0}^K (\alpha_k \cdot \mathbf{M} \cdot \mathbf{x}_{n+1-k}) + \mathbf{f}(\mathbf{x}_{n+1}) + \mathbf{b}(t_{n+1})$ 

```

---

3.2 Single shooting using BDF3

Algorithm 2 (Kvasnicka, 2020, p. 45) is based on (Kundert et al., 1990, pp. 65–70) and shows for a constant step-size  $h > 0$  an implementation to solve the BVP of the DAE (1) with the condition  $\mathbf{x}(0) = \mathbf{x}(T)$ , regarding a consistent initial value  $\mathbf{x}_0^{(0)} \in \mathbb{R}^m$ .

Here, the implementation of a single shooting is based on BDF3 and an approximate Newton method to compute the initial value  $\mathbf{x}_0^{(\ell)}$  of the  $\ell$ -th shooting iteration loop (Kvasnicka, 2020, pp. 42–45). According to (Kundert et al., 1990, pp. 65–70), the approximate sensitivity matrix  $\widehat{\mathbf{S}}(\mathbf{x}_0^{(\ell)})$  is used in line 11 of Algorithm 2 for adaption of the initial value. Therefore, in line 10, the Jacobian matrix  $\mathbf{J}_f(\mathbf{x}_{n+1})$  in accordance with equation (2) is needed. In addition, the parameter  $\text{Tol}_{abs} > 0$  specifies the accuracy of the BVP solution, according to line 3.

---

**Algorithm 2:** Solve DAE-BVP using single shooting
 

---

**Input:** DAE (1),  $\mathbf{x}_0^{(0)}$ ,  $\mathbf{J}_f : \mathbb{R}^m \rightarrow \mathbb{R}^{m \times m}$ ,  $\text{Tol}_{abs} > 0$ ,  $h > 0$ ,  
 $\mathbf{x}_N = \mathbf{x}(N \cdot h) = \mathbf{x}(T)$   
**Output:** PSS solution  $\mathbf{x}_0^{(\ell)}, \dots, \mathbf{x}_N^{(\ell)}$

- 1 Compute  $\mathbf{x}_0^{(0)}, \dots, \mathbf{x}_N^{(0)}$  according to Algorithm 1
- 2  $\ell \leftarrow 0$
- 3 **while**  $\|\mathbf{x}_N^{(\ell)} - \mathbf{x}_0^{(\ell)}\| \geq \text{Tol}_{abs}$  **do**
- 4      $\widehat{\mathbf{S}}_0(\mathbf{x}_0^{(\ell)}) \leftarrow \mathbf{I}_{m \times m}$  // assign identity matrix
- 5     **for**  $n \leftarrow 0, \dots, N-1$  **do**
- 6         **if**  $(n+1) < 3$  **then**
- 7              $K \leftarrow n+1$
- 8         **else**
- 9              $K \leftarrow 3$
- 10             // BDF coefficients as given in Algorithm 1
- 11              $\widehat{\mathbf{S}}_{n+1}(\mathbf{x}_0) \leftarrow$   
 $\left[ -\left(\frac{\alpha_0}{\beta_0 \cdot h} \cdot \mathbf{M} + \mathbf{J}_f(\mathbf{x}_{n+1})\right)^{-1} \cdot \mathbf{M} \cdot \frac{1}{\beta_0 \cdot h} \cdot \sum_{i=1}^K (\alpha_i \cdot \widehat{\mathbf{S}}_{n+1-i}(\mathbf{x}_0)) \right]$
- 12              $\widehat{\mathbf{S}}(\mathbf{x}_0^{(\ell)}) \leftarrow \widehat{\mathbf{S}}_N(\mathbf{x}_0^{(\ell)})$
- 13              $\mathbf{x}_0^{(\ell+1)} \leftarrow \mathbf{x}_0^{(\ell)} - (\widehat{\mathbf{S}}(\mathbf{x}_0^{(\ell)}) - \mathbf{I}_{m \times m})^{-1} \cdot (\mathbf{x}_N^{(\ell)} - \mathbf{x}_0^{(\ell)})$
- 14             Compute  $\mathbf{x}_0^{(\ell+1)}, \dots, \mathbf{x}_N^{(\ell+1)}$  as given in Algorithm 1
- 15              $\ell \leftarrow \ell + 1$

---

#### 4. Simulation and results

The proposed modelling and simulation strategy shall be tested on a NFC test problem consisting of two coupled loops which can be seen in [Figure 3](#). The geometry parameters from the so-called Listener 1 antenna are given in ([NFC Forum 2018](#), p. 91). On the ports of the loop antennas, matching circuits as well as source and load impedances are connected, as shown in [Figure 4](#). Additionally, the passive receiving loop antenna is loaded with a full-wave rectifier according to the standardised Listener 1 test device ([NFC Forum, 2018](#), p. 79). The conductive structure of the two coupled coils are modelled by  $b_{L,peec} = 439$  PEEC cells and  $n_{C,peec} = 441$  PEEC nodes applying the 1D PEEC method according to Section 2.1. The computation of the matrices  $\mathbf{P}$ ,  $\mathbf{L}'$  and  $\mathbf{R}'$  are implemented as proposed in ([Torchio et al., 2017](#), p. 2).

The diodes  $D_1, \dots, D_4$  are modelled as Schottky diodes BAR43S with the Shockley diode equation

$$i_D(u_D) = I_S \cdot \left( \exp\left(\frac{u_D}{\tilde{n} \cdot U_T}\right) - 1 \right),$$

using the parameters  $k_B = 1.380649 \cdot 10^{-23}$  J/K,  $T_{abs} = 300$  K,  $q_e = 1.602 \cdot 10^{-19}$  C,  $U_T = \frac{k_B \cdot T_{abs}}{q_e}$ ,  $\tilde{n} = 1.4622$  and  $I_S = 0.4345 \mu\text{A}$ .

The circuit in [Figure 4](#) is supplied by  $u_0(t) = 3V \cdot \sin(2\pi \cdot f_0 \cdot t)$ , with  $f_0 = 13.56$  MHz and can be described by DAE (1) with  $m = 1326$  unknowns. Moreover, [equation \(1\)](#) is an index-1 DAE in accordance with ([Schwarz and Tischendorf 2005](#), p. 8) because loops contain

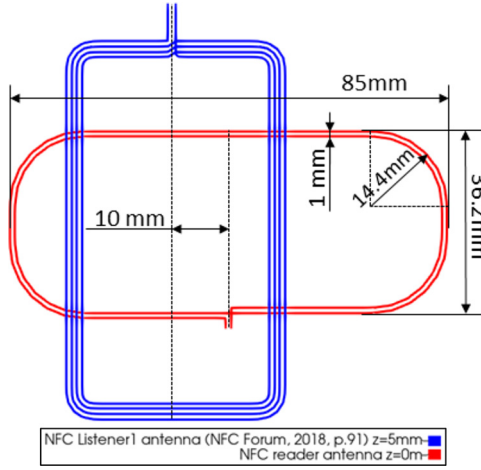


**Figure 3.**  
Geometry of NFC test  
problem

capacitive elements only, i.e. pure C-loops (e.g. loop  $\mathbf{C}_{\text{peec},1} - \mathbf{C}_{p1} - \mathbf{C}_{\text{peec},127}$ ), does not lead to a higher index. Hence, Algorithm 2 can be applied to solve the relating DAE (1). To achieve a better convergence behaviour, the implementation of Algorithm 2 was adapted on the damped Newton method like proposed in (Bank and Rose 1981, pp. 287–288). Additionally, the application of Algorithm 2 needs for  $\mathbf{u}_R = (\mathbf{u}_{R,\text{peec}}^\top, \mathbf{u}_{R,\text{ext},\text{lin}}^\top, u_{D_1}, u_{D_2}, u_{D_3}, u_{D_4})^\top$  the Jacobian matrix

$$\mathbf{J}_{\mathbf{r}_R}(\mathbf{u}_R) = \begin{pmatrix} \mathbf{R}_{\text{peec}}^{-1} & \mathbf{0} & \mathbf{0} \\ \mathbf{0} & \mathbf{R}_{\text{ext},\text{lin}}^{-1} & \mathbf{0} \\ \mathbf{0} & \mathbf{0} & \text{diag} \left( \left( \frac{di_{D_\ell}(u_{D_\ell})}{du_{D_\ell}} \right)_{1 \leq \ell \leq 4} \right) \end{pmatrix},$$

whereby  $\frac{di_{D_\ell}(u_{D_\ell})}{du_{D_\ell}} = \frac{I_S}{\bar{n} \cdot U_T} \cdot \exp\left(\frac{u_{D_\ell}}{\bar{n} \cdot U_T}\right)$  and  $\mathbf{R}_{\text{ext},\text{lin}}$  is a diagonal matrix consisting of external linear resistors.

The following computations are implemented in MATLAB<sup>®</sup>, and the simulation was run on a Windows machine equipped with a 2-cores/4-threads processor (Intel<sup>®</sup> Core<sup>™</sup> i7-6500U CPU@2.50 GHz) and 16 GB RAM.

Firstly, the functionality of the single shooting method regarding Section 3.2 is verified by transient analysis regarding Section 3.1 (Kvasnicka, 2020, pp. 73–78). Further, the proposed formulation of the coupled field-circuit problem in terms of DAE system solved by a single shooting method is verified on a linear circuit with a time-harmonic PEEC solver. Therefore, the full-wave rectifier circuit connected between nodes 128 and 441, as shown in Figure 4, is replaced by a linear load resistance  $R_{\text{lin}} = 400 \Omega$ . Hence, the load for the passive NFC test antenna is given by  $C_{p2}$  and  $R_{\text{lin}}$ , only. This linearised circuit was computed by single shooting and by a harmonic solver using the admittance method similar to (Ekman 2003, pp. 54–56). Figure 5(a) shows that the numerical computation of both methods was

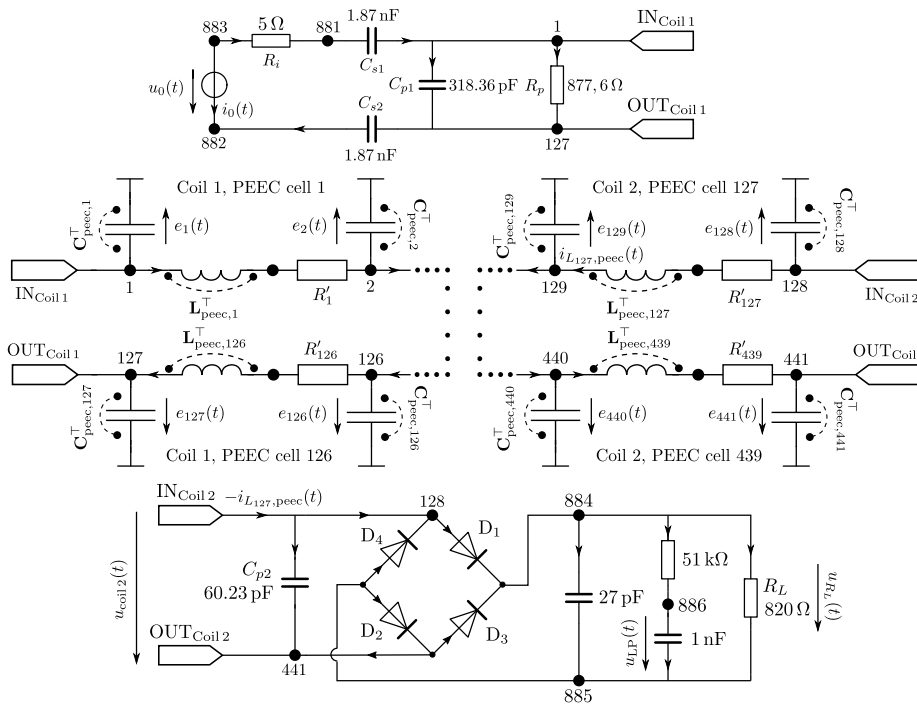


**Figure 4.** Equivalent circuit of two coupled coils using PEEC method, matching network  $C_{s1}, C_{s2}, C_{p1}, C_{p2}, R_p$  and nonlinear load containing a full-wave rectifier

highly concordant for selected signals. The runtime of the harmonic solver was 0.198s, and the single shooting method needed 121.5s, whereby two shooting iteration loops were necessary.

Finally, the signals presented in [Figure 5\(b\)](#) give some selected results for the original nonlinear test problem shown in [Figure 4](#). The runtime was 550.1s for nine necessary shooting iteration loops. In both cases, a single shooting was configured with the initial value  $\mathbf{x}_0^{(0)} = \mathbf{0}$ . Due to the different time constants in the system, the transient analysis needed more than 3400 cycle durations to compute the PSS solution. For example, for  $N = 30$  grid points per period duration, this resulted in a speedup with a shooting of about 114 ([Kvasnicka, 2020](#), pp. 74–76).

## 5. Conclusion and outlook

Based on the quasi-static PEEC method for conductive structures, the NFC problem directly coupled with a nonlinear electrical circuit could be modelled. The proposed MNA formulation is able to handle independent sources, linear elements and nonlinear resistive elements. Finally, the entire circuit is described by means of a DAE, and the computation of the PSS solution is implemented by a single shooting. The proper functionality of the single shooting method was verified on a linear test problem, and an efficient calculation of a test problem containing nonlinear resistive elements could be shown.

Further investigations could inspect the behaviour of applications using general periodic sources. Moreover, the introduced theory can be adapted by using PEEC for

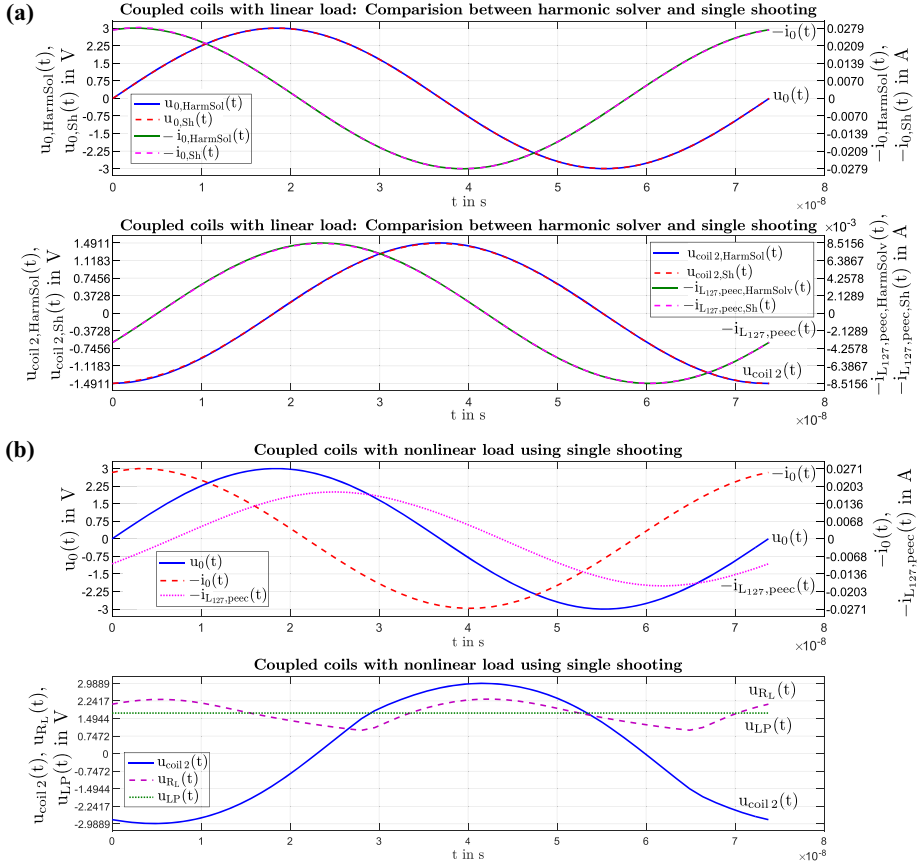


**Figure 5.** (a) Comparison between harmonic solver and single shooting for linear circuit, (b) Computation of nonlinear circuit using single shooting. Shooting was computed for  $N = 50$  grid points per period duration and  $\text{ToI}_{\text{abs}} = 10^{-5}$

dielectric or magnetic structures. With regard to higher frequencies and applications in the far-field further developments, including time retardation, become necessary.

**References**

Ascher, U.M. and Petzold, L.R. (1998), "Computer methods for ordinary differential equations and differential-algebraic equations", *Society for Industrial and Applied Mathematics*, 1st ed.  
 Bank, R.E. and Rose, D.J. (1981), "Global approximate Newton methods", *Numerische Mathematik*, Vol. 37 No. 2, pp. 279-295.  
 Bauernfeind, T., Baumgartner, P., Biró, O., Hackl, A., Magele, C., Renhart, W. and Torchio, R. (2018), "Multi-objective synthesis of NFC-transponder systems based on PEEC method", *IEEE Transactions on Magnetics*, Vol. 54 No. 3, pp. 1-4.  
 Bauernfeind, T., Baumgartner, P., Mušeljčić, E. and Torchio, R. (2020), "Challenges in the synthesis of NFC transponders", *International Compumag Society (ICS) Newsletter*, Vol. 27 No. 3, pp. 3-14.

- 
- Ekman, J. (2003), "Electromagnetic modeling using the partial element equivalent circuit method", PhD thesis, Lulea University of Technology.
- Kundert, K.S., White, J.K. and Sangiovanni-Vincentelli, A. (1990), *Steady-State Methods for Simulating Analog and Microwave Circuits*, Springer.
- Kvasnicka, S. (2020), "Berechnung des periodisch eingeschwungenen Zustands von nichtlinearen Netzwerken unter Anwendung der partial element equivalent circuit Methode", Master Thesis, Graz University of Technology.
- NFC Forum (2018), "NFC forum: NFC analog technical specification", Version 2.1, August 2018, available at: [www.nfc-forum.org](http://www.nfc-forum.org)
- Riaza, R. (2008), "Differential-algebraic systems, analytical aspects and circuit applications", *World Scientific*.
- Schwarz, D.E. and Tischendorf, C. (2005), *Structural Analysis for Electric Circuits and Consequences for MNA*, Humboldt University of Berlin.
- Torchio, R., Bettini, P. and Alotto, P. (2017), "PEEC-based analysis of complex fusion magnets during fast voltage transients with H-matrix compression", *IEEE Transactions on Magnetics*, Vol. 53 No. 6, pp. 1-4.
- Torchio, R. (2019), "Extending the unstructured PEEC method to magnetic, transient, and stochastic electromagnetic problems", PhD thesis, Università degli Studi di Padova and Université Grenoble Alpes.

**Corresponding author**

Samuel Kvasnicka can be contacted at: [samuel.kvasnicka@tugraz.at](mailto:samuel.kvasnicka@tugraz.at)